

# Robust Reinforcement Learning for Discrete Compositional Generation via General Soft Operators

**Marco Jiralerspong\***  
Université de Montréal and Mila

**Esther Derman**  
Université de Montréal and Mila

**Danilo Vucetic**  
Université de Montréal and Mila

**Nikolay Malkin**  
University of Edinburgh and CIFAR

**Bilun Sun**  
Independent

**Tianyu Zhang**  
Université de Montréal and Mila

**Pierre-Luc Bacon**  
Université de Montréal, Mila and CIFAR

**Gauthier Gidel**  
Université de Montréal, Mila and CIFAR

## Abstract

A major bottleneck in scientific discovery involves narrowing a large combinatorial set of objects, such as proteins or molecules, to a small set of promising candidates. While this process largely relies on expert knowledge, recent methods leverage reinforcement learning (RL) to enhance this filtering. They achieve this by estimating proxy reward functions from available datasets and using regularization to generate more diverse candidates. These reward functions are inherently uncertain, raising a particularly salient challenge for scientific discovery. In this work, we show that existing methods, often framed as sampling proportional to a reward function, are inadequate and yield suboptimal candidates, especially in large search spaces. To remedy this issue, we take a robust RL approach and introduce a unified operator that seeks robustness to the uncertainty of the proxy reward function. This general operator targets peakier sampling distributions while encompassing known soft RL operators. It also leads us to a novel algorithm that identifies higher-quality, diverse candidates in both synthetic and real-world tasks. Ultimately, our work offers a new, flexible perspective on discrete compositional generation tasks. Code: <https://github.com/marcojira/tgm>.

## 1 Introduction

The task of scientific discovery centers on discovering novel objects with desirable properties such as antimicrobial resistance or binding affinity. These objects are often discrete and structured such that they can be constructed through a sequence of compositional steps, e.g., proteins as sequences of amino acids, molecules composed of various smaller fragments [2, 51]. Due to this compositionality, the number of possible objects grows exponentially with object size and becomes too large to search exhaustively. On top of that, experimentally evaluating potential objects can be too technical or expensive. Nonetheless, in many cases, researchers have access to a proxy reward model that quantitatively approximates the value of the property of interest [15, 19].

\*Correspondence to [marco.jiralerspong@mila.quebec](mailto:marco.jiralerspong@mila.quebec)

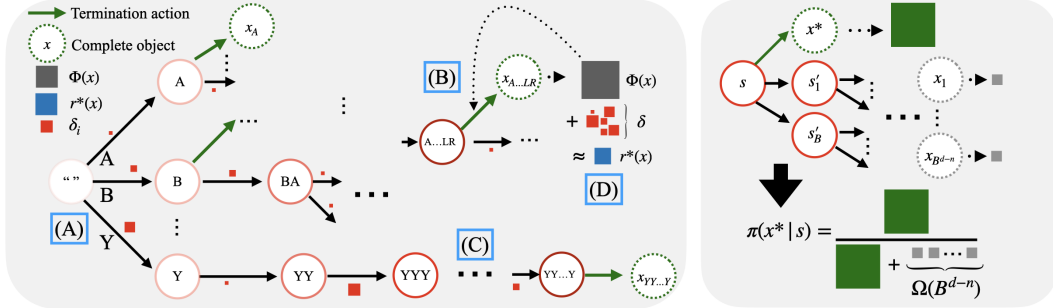


Figure 1: (Left) A DCG for a protein sequence generation task. (A) Starting from an empty string, amino acids are added sequentially until termination. (B) Then, the full sequence is evaluated by a proxy reward function  $\Phi(x)$  whose value is given as reward for the termination action. (C) Over the course of the protein generation, uncertainty accumulates through the  $\delta_i$ . (D) The true reward depends on  $\Phi(x)$  and the accumulated uncertainty. (Right) Illustrated issue with sampling proportional to reward. The much larger reward of the optimal sequence (in green) is drowned out by all the rewards in the combinatorial explosion of longer subsequences.

A large body of work leverages this proxy reward function to narrow the set of objects to a small subset of promising candidates, which can then be tested in a lab [13, 25, 54, 1]. An alternative approach that has demonstrated growing popularity and effectiveness is to pose this problem as an RL task [16, 14, 7]. In what we will denominate discrete compositional generation (DCG), the object construction process is viewed as a Markov decision process (MDP) where terminal states correspond to complete objects and yield a reward corresponding to the evaluation of that object by the proxy reward function. Then, the learned policy can be used as a generative model, ideally sampling promising candidates.

Among these approaches, generative flow networks (GFNs) have shown considerable success in various domains [5, 32, 56, 12]. GFNs learn an amortized policy and, at optimality, sample objects with probability proportional to the exponential of their reward (2). Tight connections have been established between GFNs and maximum-entropy RL, showing that this objective underpins the diversity of generated samples [49, 41, 17]. While this exact sampling goal is useful in certain applications, e.g., sampling from an intractable Bayesian posterior, it does not necessarily generate the most promising candidates.

Intuitively, if we had access to the true reward function from lab evaluations of objects, the standard RL objective, which seeks to maximize reward, could be appropriate. Regularization and the diversity it entails attempt to be robust to the uncertainty of the proxy reward function. In this work, we show an explicit connection between various forms of regularization and robustness to different forms of uncertainty. In particular, we show that regularizing by the Shannon entropy, as is typically done in GFNs, yields an *inappropriate reward constraint set* that does not contain the proxy reward. Therefore, motivated by the connection between these fields, we introduce alternative operators to address this issue and demonstrate their effectiveness.

### Our contributions:

- (1) We propose a compositional model for reward uncertainty in DCG tasks. From this model, we make explicit the connections between regularized RL and reward-robust RL on value functions, allowing us to analyze the reward uncertainty sets associated with various soft operators.
- (2) Motivated by the robust interpretation of Shannon entropy regularization in RL and the issue it raises for DCG, we introduce a unifying operator called general mellowmax (GM), that smoothly interpolates between the GFN operator and other soft RL operators. We then propose trajectory GM (TGM) as a practical algorithm for this operator.
- (3) We experimentally show that TGM performs better than GFNs and other soft RL baselines at generating diverse, high-reward objects for both synthetic and real-world sequence design tasks.

## 2 Background

**MDPs.** An MDP is a tuple  $(\mathcal{S}, \mathcal{A}, \gamma, P, r)$  where  $\mathcal{S}$  is a finite state space,  $\mathcal{A}$  a finite action space,  $\gamma \in [0, 1)$  a discount factor,  $P : \mathcal{S} \times \mathcal{A} \rightarrow \Delta_{\mathcal{S}}$  is a transition kernel and  $r : \mathcal{S} \times \mathcal{A} \rightarrow [-R, R]$  a bounded reward function. Define  $\Pi$  as the set of policy mappings  $\pi : \mathcal{S} \rightarrow \Delta_{\mathcal{A}}$ . The goal is to find  $\pi \in \Pi$  that maximizes the value function  $v_r^\pi(s) := \mathbb{E}^\pi[\sum_{t=0}^{\infty} \gamma^t r(s_t, a_t) \mid s_0 = s]$ ,  $\forall s \in \mathcal{S}$ . The dependence of the value function on the reward function is made explicit through the subscript  $r$ , as clarified in the next paragraph. For any policy  $\pi \in \Pi$ , the expected reward is  $r^\pi(s) := \sum_{a \in \mathcal{A}} \pi_s(a) r(s, a)$  and

the expected transition is  $P^\pi(s, s') := \sum_{a \in \mathcal{A}} \pi_s(a) P(s, a, s')$ . The evaluation Bellman operator given by  $T_r^\pi v := r^\pi + \gamma P^\pi v$  for all  $v \in \mathbb{R}^{\mathcal{S}}$  is known to be contracting, admitting  $v_r^\pi$  as a fixed point. Similarly, the optimal value function  $v_r^*(s) := \max_{\pi \in \Pi} v_r^\pi(s)$  is the fixed point of the optimal Bellman operator  $T_r^* v(s) := \max_{\pi \in \Pi} T_r^\pi v(s)$ ,  $\forall v \in \mathbb{R}^{\mathcal{S}}, s \in \mathcal{S}$ . An optimal policy can be derived from iterative Bellman updates, which form the building block of RL [45].

**Robust MDPs.** The true reward or transition function of an MDP is rarely known in practice. It may be estimated from trajectory data, but a small error on the MDP model can greatly alter policy performance [40]. The robust MDP setting addresses this issue by assuming that  $(P, r)$  is unknown, lying in a given uncertainty set. In our applicative setting of DCG where transitions are fully determined by the performed actions, we reasonably assume that only the reward model is uncertain and  $r \in \mathcal{R}$ . Then, we aim to maximize performance for the worst-case model, namely:

$$v_{\mathcal{R}}^\pi(s) := \min_{r \in \mathcal{R}} v_r^\pi(s), \quad \forall s \in \mathcal{S}.$$

To solve this max-min problem, one can resort to robust Bellman operators  $T_{\mathcal{R}}^\pi v := \min_{r \in \mathcal{R}} T_r^\pi v$  and  $T_{\mathcal{R}}^* v := \max_{\pi \in \Pi} T_{\mathcal{R}}^\pi v$ ,  $\forall v \in \mathbb{R}^{\mathcal{S}}$ . Indeed, both are contracting and admit the robust value function  $v_{\mathcal{R}}^\pi$  and the optimal robust value function  $v_{\mathcal{R}}^*$  as fixed points, respectively [30, 53].

**Regularized MDPs** provide a general framework for regularization in RL, recovering celebrated algorithms such as soft Q-learning [26]. A regularized MDP is an MDP  $(\mathcal{S}, \mathcal{A}, \gamma, P, r)$  combined with a family  $\Omega := (\Omega_s)_{s \in \mathcal{S}}$  of convex functions  $\Omega_s : \Delta_{\mathcal{A}} \rightarrow \mathbb{R}$ . At each state  $s \in \mathcal{S}$ ,  $\Omega_s$  defines a policy regularizer  $\Omega_s(\pi_s)$ , for  $\pi_s \in \Delta_{\mathcal{A}}$ . The regularized Bellman operator is given by:

$$[T^{\pi, \Omega} v](s) := T_r^\pi v(s) - \Omega_s(\pi_s), \quad \forall v \in \mathbb{R}^{\mathcal{S}}, s \in \mathcal{S}.$$

and its greedy equivalent by  $[T^{*, \Omega} v](s) := \max_{\pi_s \in \Delta_{\mathcal{A}}} [T^{\pi, \Omega} v](s)$  [23]. [18] have established an equivalence between policy-regularized and robust Bellman operators, thus highlighting a formal motivation for regularized RL. The statement below is a direct reformulation of [18, Thm. 3.1].

**Theorem 2.1** ([18]). *Assume that the reward function  $r$  is uncertain and satisfies  $r_s \in \mathcal{R}_s := r_0(s, \cdot) + \tilde{\mathcal{R}}_s$ , where  $\tilde{\mathcal{R}}_s \subseteq [-R, R]^{\mathcal{A}}$  is closed and convex for all  $s \in \mathcal{S}$ . Then, for any  $\pi \in \Pi$ , the robust value function  $v_{\mathcal{R}}^\pi$  is the fixed point of the regularized Bellman operator  $T^{\pi, \Omega}$  with  $\Omega_s(\pi_s) := \max_{r_s \in \tilde{\mathcal{R}}_s} \langle -\pi_s, r_s \rangle$ . In other words, it holds that  $v_{\mathcal{R}}^\pi(s) = T_{r_0}^\pi v_{\mathcal{R}}^\pi(s) - \Omega_s(\pi_s)$ ,  $\forall s \in \mathcal{S}$ .*

**DCGs** are special instances of standard MDPs with deterministic transitions. They can fully be described by a tuple  $(\mathcal{G}, \Phi)$ , where  $\mathcal{G}$  is a directed acyclic graph with a single source state  $s_0$  and a set of terminal states  $\mathcal{X}$  (see Fig. 1). Each node in the graph corresponds to a set of parts,  $s_0$  being the empty set. An edge  $(s \rightarrow s')$  represents either adding a part to the set  $s$  to get  $s'$  or a termination action if  $s' \in \mathcal{X}$ . Each completed object  $x \in \mathcal{X}$  has an associated reward  $\beta \Phi(x)$  given by the proxy reward model  $\Phi : \mathcal{X} \rightarrow \mathbb{R}$  and  $\beta$  is a hyperparameter multiplying the reward.

Unlike in standard RL where the goal is to maximize the discounted cumulative reward, for scientific discovery we are interested in finding the most promising set of  $k$  candidates that are sufficiently distinct from one another [31]. In practice, an imperfect (but computationally efficient) proxy is used to estimate the usefulness of the candidates. That is why it can be problematic to solely search for a candidate that maximizes usefulness. Instead, given some metric  $d$  between completed objects, practitioners aim to approximately find a diverse and novel (w.r.t., the training set) set of candidates  $\{x_1, \dots, x_k\}$  with a high score [31]. Given a proxy score  $\Phi$  and a distance  $d$ , we formalize this problem as,<sup>2</sup>

$$\max_{\{x_1, \dots, x_k\} \subset \mathcal{X}} \sum_{i=1}^k \Phi(x_i) \quad \text{subject to} \quad d(x_i, x_j) > \delta, \quad \forall i \neq j. \quad (1)$$

### 3 Motivation: Limitations of GFlowNets in scientific discovery

Under a GFN perspective, the exponential of the proxy reward function can be viewed as an unnormalized probability mass. Then, the goal is to learn a per-state policy  $\pi_s$  whose sequential application samples objects proportionally to this function. Formally, if we denote by  $\mathcal{T}(x)$  all

<sup>2</sup>For simplicity, we only formalize the diversity constraint.

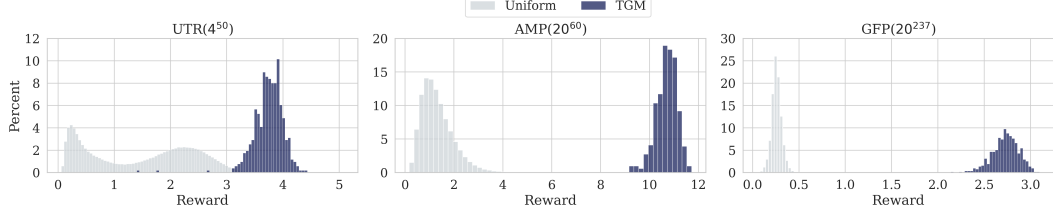


Figure 2: Distribution of  $e^{\Phi(x)}$  from 1 million uniformly drawn samples for various tasks compared to the distribution of  $e^{\Phi(x)}$  sampled by TGM at the end of training.

trajectories in  $\mathcal{G}$  ending at terminal state  $x \in \mathcal{X}$  and  $\pi_{\tau(x)}$  the probability of picking all edges from a trajectory  $\tau(x)$  under policy  $\pi$ , the objective is to sample from:

$$p(x) := \sum_{\tau(x) \in \mathcal{T}(x)} \pi_{\tau(x)} \propto e^{\beta \Phi(x)}, \quad \forall x \in \mathcal{X}. \quad (2)$$

where  $\beta$  is the reward exponent hyperparameter. We argue that this objective is suboptimal in the case of scientific discovery aiming at solving (1).

**Motivating example.** The main issue with (2) is that it yields a distribution that assigns higher probability to a large number of suboptimal reward objects rather than to a small number of high-reward objects. To demonstrate this, consider a DCG where the goal is to generate sequences of maximum length  $d$  from a vocabulary of size  $B$ . Suppose a sampler is at an optimal sequence  $s^*$  of length  $n < d$ . The sampler’s policy then needs to decide between either terminating and returning  $x^*$ , or adding more tokens and harming the usefulness of the sequence.

In doing so, it weighs  $e^{\Phi(x^*)}$  against the reward of all sequences in  $\mathcal{X}(s) = \{x : x[1:n] = s\}$  (i.e., all sequences starting with  $s$ ). There are  $|\mathcal{X}(s)| > B^{d-n}$  such sequences, and most are likely to have non-negligible rewards (see Fig. 1). As such, if the sampler perfectly matches (2),  $\pi(x^* | s) = \mathcal{O}(B^{n-d})$  and the probability of returning the optimal sequence at  $s$  decreases exponentially in  $d - n$ . The problem is apparent in many applications, as *almost all objects have non-negligible reward* (see Fig. 2). When these empirical distributions are representative, a GFN trained to optimality may conservatively estimate the probability of sampling a mode.

## 4 Robust reinforcement learning for discrete compositional generation

Training GFNs is known to be equivalent to solving an MDP regularized by the negative Shannon entropy in the autoregressive case [41, 49, 17]. Moreover, based on Thm. 2.1, entropy-regularized MDPs are equivalent to robust MDPs with uncertain reward. Yet, despite strong connections between RL and GFNs, the two settings admit different motivations and interpretations. The former uses statistical inference to perform *optimal control*, whereas the latter controls token generation to achieve *optimal samples*.

We seek to connect robust RL and GFNs for DCGs. To do so, we conceptually consider a *hidden true reward*  $r^*$  that we would like to maximize<sup>3</sup> or more exactly, a hidden reward function  $r^*$  for which we aim to find a maximizing argument. However, this reward is too expensive to compute for more than a handful of samples. Instead, we propose to robustly maximize the proxy reward  $\Phi$  accounting for the difference  $\delta$  between  $\Phi$  and  $r^*$ . Thus, the goal is to solve:

$$\max_{p \in \Delta_{\mathcal{X}}} \min_{\delta \in \mathcal{R}} \mathbb{E}_{x \sim p} [\Phi(x) + \delta(x)] \quad (3)$$

where  $\mathcal{R} \in \mathbb{R}^{|\mathcal{X}|}$  is the uncertainty set. The question then remains of how this uncertainty should be modeled in  $\mathcal{G}$ . Traditionally, the reward in a DCG is identically 0 everywhere except for terminating actions. However, assuming that uncertainty only exists at the last action misses the compositional nature of the task. Instead, we propose to decompose  $\delta(x)$  into a sum of perturbations occurring at each step of the generation process. More precisely, given a trajectory  $s_0 \xrightarrow{a_0} \dots \xrightarrow{a_{n-1}} s_n = x$ , we

<sup>3</sup>This reward would correspond to the effective properties of interest measured in a lab.

have

$$\delta(x) = \sum_{i=0}^n \delta_i[a_i] \quad \text{where } \delta_i \in \mathcal{R}_{s_i}. \quad (4)$$

In this formulation, the uncertainty on  $\Phi$  is *split between all actions taken to construct the object*, instead of only existing at the final action. From a robust RL perspective, this uncertainty set structure corresponds to the common assumption of state-rectangularity [53, 21]. However, unlike RL, which aims at optimal control, our goal is to sample promising candidates. Thus, to avoid the limitations described in § 3 and ultimately obtain better empirical performance, we need to better understand the robust interpretation of GFN objectives. In the next section, we characterize the reward uncertainty set for an arbitrary convex regularizer. Specific choices of regularizers recover the standard GFN objective (2), while others motivate a new trajectory-balance loss for discovering more promising candidates during DCG training.

#### 4.1 Fenchel-robust formulation of regularized MDPs

In this subsection, we use the robust MDP notations introduced in § 2. For any  $s \in \mathcal{S}$ , let  $f_s : \Delta_{\mathcal{A}} \rightarrow \mathbb{R}$  be a proper convex function, whose convex conjugate  $f_s^*$  is known to be proper and convex [6]. The following result provides an explicit mapping between reward-robust MDPs, as defined in (4), and regularized MDPs, through equivalent value functions.

**Theorem 4.1** (Fenchel-Robust MDP). *For any  $s \in \mathcal{S}$ , define the reward set*

$$\mathcal{R}_s := r_0(s, \cdot) + \{r_s \in \mathbb{R}^{\mathcal{A}} : f_s^*(-r_s) \leq 0\},$$

*and the regularization function  $\Omega_s(\pi_s) := f_s(\pi_s)$ ,  $\forall s \in \mathcal{S}$ . Then, for any  $\pi \in \Pi, v \in \mathbb{R}^{\mathcal{S}}$ ,  $T_{\mathcal{R}}^{\pi} v = T^{\pi, \Omega} v$ ,  $v_{\mathcal{R}}^{\pi} = v^{\pi, \Omega}$ .*

The interpretation of this theorem is that solving (3) is equivalent to solving an associated regularized MDP. Thm. 4.1 uses convex conjugacy in the context of dynamic programming. Similar results may be found in previous works [20, 29, 9, 18], but they do not directly apply to our setting. [20] focus on Shannon entropy while we encompass a broad class of regularizers. [29, 9] analyze robustness from the LP-dual perspective of RL. Although equivalent at optimum, this approach may not hold for any given policy. The notion of occupancy measure is also obscure in the context of DCG where transitions are fully determined by the agent’s decisions and the time horizon is finite. Differently, Thm. 4.1 establishes a robustness-regularization equivalence for any policy via Bellman evaluation operators. It thus provides a principled identity between robust dynamic programming in the sense of [30] and regularized MDPs in the sense of [23]. Finally, the research motivation of [18] being different, they proceed the opposite way from ours: they deduce a regularizer from generic uncertainty sets, whereas we deduce uncertainty sets from generic regularizers. This enables us to clarify the robustness properties caused by regularization.

#### 4.2 Robust sets induced by common regularizers

In this section, we analyze the uncertainty sets corresponding to common regularizers. To this aim, we introduce an interpolated regularization function between Shannon entropy and KL divergence. Not only does it encompass the above regularizers as particular cases, but it also trades off their respective effects. Given a distribution  $d_s \in \Delta_{\mathcal{A}}$ , we define the **general mellowmax (GM)** regularizer as:

$$\Omega_s^q(\pi_s) := \frac{1}{\omega_s} [\text{qKL}(\pi_s, d_s) + (1 - q)(-\text{H}(\pi_s))] \quad , \quad \forall s \in \mathcal{S}, \pi_s \in \Delta_{\mathcal{A}}, \omega_s \in \mathbb{R}_{>0}, q \in [0, 1]. \quad (5)$$

Setting  $q = 0$  leads to negative entropy regularization, while  $q = 1$  recovers the KL divergence. In particular, the optimal regularized Bellman operator associated with the uniform distribution  $d_s \equiv 1/|\mathcal{A}|$  corresponds to the mellowmax operator of [3] (see also [23]), while if we fix a  $Q$ -value estimate  $\bar{Q} \in \mathbb{R}^{\mathcal{S} \times \mathcal{A}}$  and take the softmax distribution  $d_s = \sigma_{\alpha_s}(\bar{Q}_s)$  with  $\alpha_s \in \mathbb{R}$ , the optimal operator recovers the soft mellowmax of [22]. Alternatively, the soft mellowmax with  $\alpha_s = 0$  is equivalent to mellowmax. We also observe that  $\Omega_s^q$  is equivalent to a KL between a policy and a tilted softmax, as stated below.

**Proposition 4.1.** *For all  $q \in [0, 1]$ ,  $\Omega_s^q(\pi_s) = \frac{1}{\omega_s} \text{KL}(\pi_s, d_s^{(q)}) - \frac{1}{\omega_s} \log(Z_q(d_s))$ , where  $Z_q(d_s) := \sum_{a \in \mathcal{A}} d_s(a)^q$  and  $d_s^{(q)} = d_s^q / Z_q(d_s)$  is the  $q$ -tilted softmax distribution.*

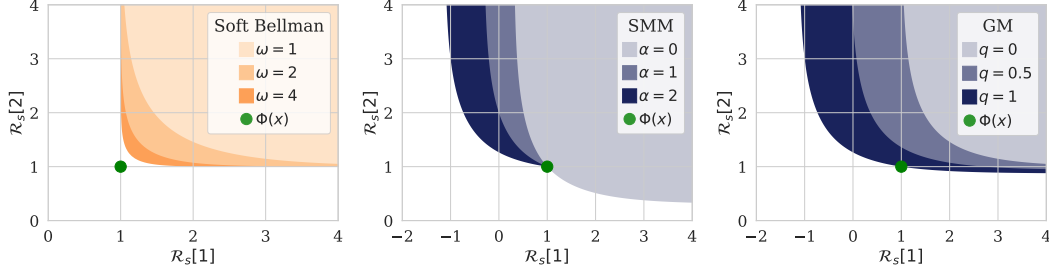


Figure 3: (Left) Uncertainty sets associated with the regularized Bellman operator for various values of  $\omega$ . Regardless of  $\omega$ , the uncertainty set *never* contains  $\Phi(x)$ . As a result, the operator is only robust to increases in reward. (Middle) Uncertainty sets associated with the soft mellowmax operator for different values of  $\alpha$  with  $d_s[1] > d_s[2]$ . For each, the uncertainty set contains  $\Phi(x)$ , yielding an operator that is robust to decreases in reward of one object (but not both at the same time). (Right) Uncertainty sets for GM. Varying  $q$  interpolates between the uncertainty sets of both operators.

Our interpolated regularizer captures three important soft RL operators and allows us to smoothly interpolate between them using  $q$  and  $\alpha_s$ . On the one hand,  $q$  tradeoffs between maximizing the policy’s entropy and having a policy that is close to the softmax of the  $Q$ -values. On the other hand,  $\alpha_s$  controls between putting more weight on actions with high  $\bar{Q}_s$ -values ( $\alpha_s > 0$ ), with low  $\bar{Q}_s$ -values ( $\alpha_s < 0$ ) or uniform weight across actions ( $\alpha_s = 0$ ). The regularized value induced by this interpolated divergence is equivalent to the robust value for

$$\mathcal{R}_s := r_0(s, \cdot) + \left\{ r_s \in \mathbb{R}^A : \frac{1}{\omega_s} \sum_{a \in A} d_s(a)^q e^{-\omega_s r_s(a)} \leq 1 \right\}. \quad (6)$$

A proof is in App. A.4. As opposed to [18], the fact that our uncertainty sets are state-rectangular makes them independent of the executed policy, so the resulting formulation fits with the original robust MDP setting [53].

We now illustrate in Fig. 3 the uncertainty sets induced by three regularizers: negative Shannon entropy, soft mellowmax, and GM. For this illustration, we consider a single-step generation process with 2 possible objects and associated proxy rewards  $[1, 1]$ . Similarly to [9], we find that the entropy regularized Bellman operator (left) fails to capture a meaningful notion of robustness. Regardless of the value of  $\omega$ , the uncertainty set does not contain  $\Phi(x)$ , though higher values of  $\omega$  do bring the set closer to the proxy rewards. In App. B, we show that this problem is significantly exacerbated in a DCG with multiple steps.

The soft mellowmax operator (middle) is guaranteed to contain  $\Phi(x)$  and illustrates a tradeoff in robustness: the true reward can be lower for one object but not both. When  $\alpha = 0$  (mellowmax), there is a symmetry in this tradeoff while increasing  $\alpha$  skews it such that the object with higher  $d_s$  only admits a small decrease in reward. One could imagine using a reference model as  $d_s$ . Then, the operator would need to be less robust to objects that have higher likelihood and very robust to unlikely objects. Finally, GM (right) interpolates between the two effects: while the uncertainty set for  $0 < q < 1$  does not contain  $\Phi(x)$ , it does contain points corresponding to decreases in reward.

## 5 Trajectory general mellowmax

Using the interpolated divergence in (5) we explicitly derive the associated operator when  $d_s = \sigma_\alpha(\bar{Q}_s)$ , which we denote by  $\pi_s^\alpha$ :

$$\Omega_{\pi_s^\alpha, s}^{\mathbf{q},*}(Q_s) := \max_{\pi_s} \langle \pi_s, Q_s \rangle - \frac{1}{\omega} \Omega_{\pi_s^\alpha, s}^{\mathbf{q}}(\pi_s) = \frac{1}{\omega} \log \left[ \langle (\pi_s^\alpha)^{\mathbf{q}}, e^{\omega_s Q_s} \rangle \right]. \quad (7)$$

The operator can be derived by finding the convex conjugate of the regularizer  $\Omega_{\pi_s^\alpha, s}^{\mathbf{q}}(\pi_s)$  through an infimal convolution of its component functions. Based on [23], the optimal regularized policy is then:

$$\pi_{\pi_s^\alpha, s}^{\mathbf{q},*}(a) = [\nabla \Omega_{\pi_s^\alpha, s}^{\mathbf{q},*}(Q_s)](a) = \frac{e^{\omega Q_s(a) + q\alpha \bar{Q}_s(a)}}{\sum_{a'} e^{\omega Q_s(a') + q\alpha \bar{Q}_s(a')}}.$$

Importantly, in DCGs, the lack of cycles implies that  $\nabla_{\pi_s} Q_s = 0$ . As such, (7) holds *even* for  $\bar{Q}_s = Q_s$  (see App. C.1). This property motivates being able to apply the GM operator both on-policy and off-policy.

**Trajectory constraints.** Instead of training on transitions, it is possible to leverage trajectory-level constraints that relate policy/value functions over multiple steps to recover training algorithms that use subtrajectories as data units. In soft RL, this connection was first formalized in [43] through path consistency learning (PCL) for maximum entropy RL. Path consistency objectives has since been derived for Tsallis entropy [10] as well as the general class of  $\alpha$ -divergences [9].

Trajectory-level constraints have been shown to be crucial to the performance of methods in DCG tasks. Trajectory balance (TB) [39] and subtrajectory balance [38] are consistently used in GFNs as DCG tasks only have terminal rewards. By connecting the policy at early states to this terminal reward, these constraints are noticeably better at propagating signal and thus improving credit assignment.

**Trajectory general mellowmax (TGM).** We now instantiate the robust RL framework discussed above in a practical algorithm for use in DCGs. Trajectory general mellowmax consists of 3 ingredients:

- (1) Using the general mellowmax operator with  $d_s = \sigma_\alpha(Q_s)$ . This setting allows us to use TGM both on-policy and off-policy and does not require a separate  $d_s$ . Instead, the policy seeks to maximize reward while being close to a softmax of the learned Q-values.
- (2) Aiming to satisfy a novel trajectory constraint derived in App. C.2. Doing so recovers the benefits of trajectory constraints for DCGs. We note that it is straightforward to derive the equivalent subtrajectory constraint.
- (3) Training a single network  $Q_\theta$  of Q-values through the VarGrad objective of [46, 55]. It can be shown that minimizing the trajectory constraint (9) is equivalent to minimizing the following loss:

$$\mathcal{L}_{\text{TGM}, Q_\theta}(\tau) = \text{Var} \left[ \frac{1}{\omega} \left( \sum_{i=1}^n \log \sigma_{q\alpha+\omega}[Q_{\theta, s_i}(a_i)] - q \log \sigma_\alpha[Q_{\theta, s_i}(a_i)] \right) - r(x) \right].$$

The simplification is helpful when sweeping over  $\beta$  as we no longer need to learn  $v_{s_0}$ . From  $Q_\theta$ , the optimal policy is easily computed.

**Theorem 5.1** (Trajectory GM). *For any DCG  $(\mathcal{G}, \Phi)$ , let  $(v^*, \pi^*)$  be the unique optimal value/policy functions for the GM operator with  $v_x^* = 0$  for all  $x \in \mathcal{X}$ . Then, for a given Q-function  $\tilde{Q}$ ,*

$$\sigma_{q\alpha+\omega}(\tilde{Q}_s) = \arg \max_{\pi_s} \langle \pi_s, Q_s \rangle - \frac{1}{\omega} \Omega_{\sigma_\alpha(Q_s), s}^q(\pi_s), \quad (8)$$

*holds for all states  $s$  if and only if*

$$v_0^* + \sum_{i=0}^n \frac{1}{\omega} \underbrace{\left( \log \sigma_{q\alpha+\omega}(\tilde{Q}_{s_i})[a_i] - q \log \sigma_\alpha(\tilde{Q}_{s_i})[a_i] \right)}_{g(\tilde{Q}_{s_i}, a_i)} - r(s_i, a_i) = 0, \quad (9)$$

*holds for all full trajectories  $s_0 \xrightarrow{a_0} \dots \xrightarrow{a_{n-1}} s_n \xrightarrow{a_n} x$  in the DCG.*

In particular, Thm 5.1 explicits that satisfying the trajectory constraint (9) on all trajectories yields  $Q_\theta$  such that  $\sigma_{q\alpha+\omega}(Q_\theta)$  is the optimal policy for the regularized problem. See App. C.2 for the proof.

## 6 Related work

Historically, the goal of sampling proportional to reward was tackled by Markov chain Monte Carlo (MCMC) methods [24]. These methods construct chains through a random walk: from a set of initial points, new points are proposed and either accepted or rejected based on their function value (in this case, their proxy reward). While theoretically appealing, these methods struggle in high dimensions, particularly when it comes to discovering separate modes, as discussed in [5].

On the other hand, GFNs have had demonstrated success in areas including protein design [31], drug discovery [48], and material design [1]. Currently, the standard way of dealing with the excessive smoothness of GFN policies is through temperature conditioning [55, 35, 56]. The GFN target can be posed more generally as learning  $p(x) \propto r(x)^\beta$  where higher  $\beta$  yields peakier policies. Temperature conditioning involves learning a policy that is conditional on  $\beta$  and varying

$\beta$  throughout training. Note this approach complements ours, as temperature conditioning can also be used in our framework. [42] has also proposed a dynamic regularization coefficient (based on the number of actions) for maximum entropy RL which could also be used to address excessive smoothness for GFNs (similarly to varying  $\omega_s$  in our framework).

Alternatively, many RL methods fit inside the regularized RL framework of [23]. [42] studies modifying entropy with a dynamic temperature coefficient to attempt to address excessive regularization. Other forms of regularization and their corresponding operators have also been proposed including the mellowmax [3] operator which takes the log-mean-exp of Q-values instead of the log-sum-exp. [33] uses an adversarial version of the mellowmax operator to develop AFlowNets. The operator has since been extended to the soft mellowmax operator [22]. Our contribution with respect to these works relies on connecting them to DCGs, generalizing them and integrating them with trajectory constraints to successfully apply them to real DCG tasks.

## 7 Experiments

Our experiments are aimed at answering the following questions:

- [Q1] How does the parameter  $q$  affect the peakiness of sampling in small and synthetic environments?
- [Q2] Does TGM find better candidates than standard methods in large biological design DCG tasks?
- [Q3] How robust is TGM to changes in hyperparameter settings?

### 7.1 Impact of $q$ in small and synthetic environments [Q1]

**TF-Bind-8.** Originally proposed in [50], TF-Bind-8 generates DNA sequences of length 8 to find those with high binding activity to human transcription factors. The reward is the known experimental binding activity of the sequence from [4]. As there are only  $4^8$  such sequences, the search space is small enough to compute the optimal value for each operator (through backward recursion). We compare the optimal sampling densities of each algorithm in Fig. 4 for  $\beta = 4$ ,  $\alpha = 2$  and  $\omega = 2$ . There is a noticeable qualitative difference between both sampling distributions. The optimal GFN sampler still assigns most of its mass to samples that yield slightly better than the average reward. On the other hand, most of the mass of the optimal TGM samplers are at rewards above 0.8. It takes  $\beta = 16$  for GFNs to match the TGM sampling.

**Bit sequence.** The bit sequence task is significantly larger with  $2^{120}$  possible sequences and follows the protocol proposed in [39]. The goal is to generate bit sequences of length  $n$  by adding  $k$  bits at a time.  $M$  modes are selected semi-randomly and the reward is given by  $r(x) = 1 - \min_{y \in M} d(x, y)/n$  where  $d$  is the Levenshtein edit distance [37]. Loosely, the reward of a sequence is the negative normalized edit distance to the nearest mode.

As we have access to the ground-truth modes in this case, we evaluate methods according to the following metrics: (1) the number of modes found, where a mode is deemed found if a sample is generated within distance  $\delta = 28$  of that mode; (2) for each mode, we track the distance to the closest sample generated during training. We report the average of this number over the  $M$  modes.

For each algorithm, we report the performance of the best hyperparameters based on the final average minimum distance at the end of training. See App. D.3 for further details. While the best GFN run is able to match  $q = 0$ , the increased peakiness of non-zero values of  $q$  yields noticeable benefits. The best-performing runs of  $q > 0$  find samples that are much closer to the modes *while also discovering more of them*. The increased peakiness of the sampling does not seem to alter mode diversity.

### 7.2 Biological sequence design [Q2]

We now focus on tasks based on real-world domains with proxy reward functions trained on actual datasets. The tasks are based on the setup of [39] and use the datasets from [50]. For each, a transformer  $\Phi$  is first trained (either for classification or regression) on the respective training set. Then, the mean and standard deviation of the transformer’s output is computed using the validation set. Before being used as a proxy reward, the transformer output is normalized. See App. D.4 for more details.



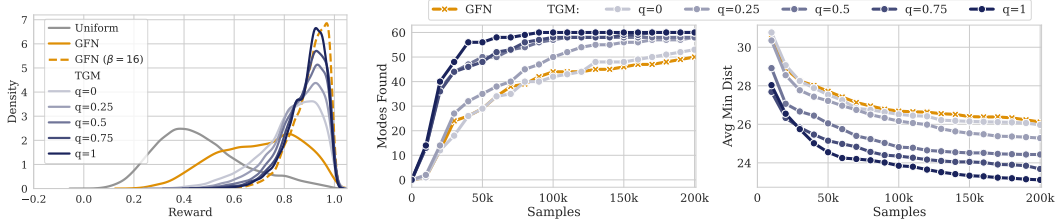


Figure 4: (Left) Comparison of the optimal sampling distribution of GFN and variants of TGM for TF-Bind-8 rewards. For the same  $\beta = 4$ , TGM concentrates significantly more mass on the upper quantiles of the reward distribution. (Middle) Number of modes found by TGM and GFN. The increased peakiness of the TGM sampling does not harm its ability to find different modes. (Right) Average (over modes) of the distance of the closest sample found for each mode. On average, increasing  $q$  allows TGM to find closer samples to the true modes.

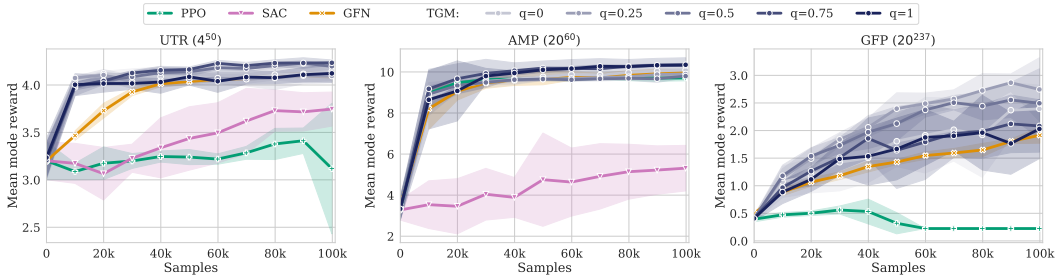


Figure 5: Mean mode reward during training of TGM compared to baselines on the biological sequence design tasks. The graph shows the average and standard deviation (shaded area) for each method over five different seeds. In all domains, variants of TGM either match or outperform GFN/PPO/SAC with a particularly pronounced difference in GFP, the largest domain.

### 7.2.1 Setting and tasks

**5' Untranslated Region Sequence (UTR).** 5' UTR is an mRNA region that regulates transcription of the main coding sequence. The goal of the task is to find a UTR sequence of length 50 that maximizes predicted gene expression level. We take the dataset of 280 000 filtered sequences from [50] and associated ribosome loads. We train a transformer as regressor to predict the ribosome load from a sequence. The vocabulary consists of 4 nucleotides.

**Antimicrobial Peptide (AMP).** Antimicrobial peptides are short sequences of amino acids that have effects on microbes (bacteria, viruses, etc.). The goal of this task is to discover novel peptides that are likely to have antimicrobial properties. The DBAASP database [44] has collected known peptides with and without antimicrobial activity. We use the dataset (sourced from [50]) of 9222 non-AMP sequences and 6438 AMP sequences and train a binary classifier (predicting whether a sequence has antimicrobial properties or not). We use the normalized logit of the classifier as proxy reward. The vocabulary for this task consists of the 20 amino acids, plus a token corresponding to sequence termination. We mask the tokens such that the minimum sequence length is 14 and the maximum sequence length is 60. This is the only task where we allow variable length sequences (as it is the only one whose dataset contains sequences of variable length).

**Green Fluorescent Protein (GFP).** The green fluorescent protein is a length 237 protein whose fluorescence has numerous applications in biology. The goal of this task is to discovery other proteins with high predicted fluorescence. We take the processed dataset from [50] which contains 56086 variations of the original sequence and their measured fluorescence. We train a regressor to predict the measured fluorescence and the vocabulary consists of the 20 amino acids.

**Evaluation.** Each method is trained for 100 000 generated samples after which we evaluate the learned network. By varying the temperature coefficient of the policy, we can move along a quality / diversity curve for each sampler. Thus, at test time we generate a set of samples for a range of temperature coefficients. We then aggregate the samples and aim to approximately determine the best  $k$  distinct samples (i.e., such that the minimum distance is  $\delta$ ) found by the policy. While this problem is NP-complete [34] (it can be seen as an instance of finding a maximal independent set), a greedy approach appears to work well in practice. For each method, a sweep is performed over

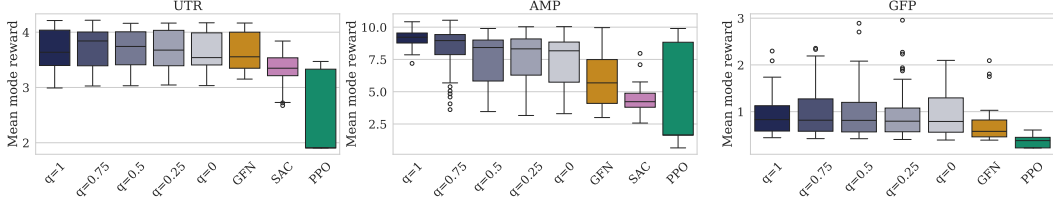


Figure 6: Spread of final mean mode rewards for various algorithms from a grid sweep over learning rates,  $\beta$  and  $\omega$ . TGM on average performs better in AMP and GFN and similarly in UTR.

hyperparameters. The best performing setting (based on final mean mode reward) is then run with 5 different seeds. See App. D.4 for further details on training/evaluation.

**Results.** For all three tasks, *all variants of TGM either roughly match or exceed the performance of GFN, soft actor-critic (SAC) [27] and proximal policy optimization (PPO) [47]*. Similarly to what was found in [39, 38], SAC and PPO perform relatively poorly. We hypothesize that the credit assignment problem from terminal rewards is a significant issue for these methods. In AMP, where generating shorter sequences is possible, PPO is able to achieve similar results to TGM/GFN. The difference between TGM and GFN is most pronounced in the largest environment GFP, where TGM nearly doubles the mean mode reward and finds modes with significantly higher reward than the mean in Fig. 2, at the expense of increased variance. We hope this result shows the potential scalability of TGM, although more work would be needed to confirm this. Interestingly, the effect of  $q$  is more varied in these environments, showing the benefits of interpolation in the GM operator. The best performing variants use  $q \in (0, 1)$ . The additional entropy bonus of lower  $q$  values appears to be aiding either policy exploration during training or the diversity of generated samples.

### 7.3 Hyperparameter robustness [Q3]

The best runs for Fig. 5 were selected from grid sweep over learning rates  $\{0.00001, 0.0001, 0.001\}$ ,  $\beta \in \{4, 16, 64, 256\}$  and inverse temperature parameters  $\omega \in \{1, 4, 16\}$ . For SAC and PPO, we set the entropy coefficient to  $1/\omega$ . For GFN, we set the sampling temperature of the policy to  $1/\omega$ . To ensure an equal number of runs per method, we fix  $\alpha = 1$  and only vary  $\omega$  for TGM, although, varying  $\alpha$  as well would likely be beneficial.

TGM variants seem robust to these hyperparameter variations. The average SAC run is relatively stable at lower performance values, while PPO is very sensitive to hyperparameter settings, with the best runs achieving strong performance in AMP. *The average mean mode reward of TGM is higher than GFN across  $q$  and environments.* For UTR, the spread between runs of TGM and GFN is relatively small with GFN having a slightly better worst-case performance. For AMP, average performance is good, although the worst TGM/GFN runs perform significantly worse. Notably,  $q = 1$  has little variability with almost all well-performing runs. Finally, for GFP, there is significantly more variability with the best performances coming from outliers for each method.

## 8 Conclusion

In this paper, we adapt the reward-robust RL framework to DCG tasks where rewards are given for entire trajectories. Then, motivated by the inadequacy of sampling proportional to reward, we generalize various soft RL operators and propose GM as an interpolated regularizer. From this regularizer, we develop a novel algorithm (TGM) and show it is consistently able to outperform GFNs on a variety of DCG tasks. Ultimately, we believe TGM has the potential to be a more general and effective framework for finding promising candidates in discrete compositional generation tasks.

**Limitations.** This work only focuses on DCG tasks, and particularly autoregressive generation, where the DCG has a tree structure. We have not discussed general DAGs where nodes can have multiple parents. In addition, the contribution of this work is algorithmic in nature, showing the ability to learn sequential samplers for any given proxy reward function. We do not focus on the generalization abilities of the tested proxy reward function and the actual design of promising DNA/protein sequences. We also do not focus on uncertainty sets that leverage some properties of the proxy (e.g., the proxy could be more confident in certain candidates).

## 9 Acknowledgments

The authors would like to thank Glen Berseth, Muqeeth Mohammed and Sobhan Mohammadpour for fruitful discussions and feedback as well as Moksh Jain for providing helpful advice for setting up the biological sequence/bit sequence experiments. This research was enabled in part by compute resources provided by Mila. G. Gidel is a CIFAR AI Chair, he is supported by a Discovery Grant from the Natural Science and Engineering Research Council (NSERC) of Canada. M. Jiralespong is supported by an IVADO fund under the Canada First Research Excellence Fund grant to develop robust, reasoning, and responsible artificial intelligence. E. Derman is supported by Samsung. M. Jiralespong acknowledges the support of the Natural Sciences and Engineering Research Council of Canada (NSERC) [funding reference no. 600916].

## References

- [1] M. AI4Science, A. Hernandez-Garcia, A. Duval, A. Volokhova, Y. Bengio, D. Sharma, P. L. Carrier, Y. Benabed, M. Koziarski, and V. Schmidt. Crystal-GFN: sampling crystals with desirable properties and constraints. *arXiv preprint 2310.04925*, 2023.
- [2] C. Angermueller, D. Dohan, D. Belanger, R. Deshpande, K. Murphy, and L. Colwell. Model-based reinforcement learning for biological sequence design. In *International Conference on Learning Representations (ICLR)*, 2019.
- [3] K. Asadi and M. L. Littman. An alternative softmax operator for reinforcement learning. In *International Conference on Machine Learning (ICML)*, 2017.
- [4] L. A. Barrera, A. Vedenko, J. V. Kurland, J. M. Rogers, S. S. Gisselbrecht, E. J. Rossin, J. Woodard, L. Mariani, K. H. Kock, S. Inukai, et al. Survey of variation in human transcription factors reveals prevalent DNA binding changes. *Science*, 351(6280):1450–1454, 2016.
- [5] E. Bengio, M. Jain, M. Korablyov, D. Precup, and Y. Bengio. Flow network based generative models for non-iterative diverse candidate generation. *Neural Information Processing Systems (NeurIPS)*, 2021.
- [6] D. Bertsekas. *Convex optimization theory*, volume 1. Athena Scientific, 2009.
- [7] A. Bou, M. Thomas, S. Dittert, C. Navarro, M. Majewski, Y. Wang, S. Patel, G. Tresadern, M. Ahmad, V. Moens, et al. ACEGEN: Reinforcement learning of generative chemical agents for drug discovery. *Journal of Chemical Information and Modeling*, 64(15):5900–5911, 2024.
- [8] J. Bradbury, R. Frostig, P. Hawkins, M. J. Johnson, C. Leary, D. Maclaurin, G. Necula, A. Paszke, J. VanderPlas, S. Wanderman-Milne, and Q. Zhang. JAX: composable transformations of Python+NumPy programs, 2018. URL <http://github.com/jax-ml/jax>.
- [9] R. Brekelmans, T. Genewein, J. Grau-Moya, G. Delétang, M. Kunesch, S. Legg, and P. Ortega. Your policy regularizer is secretly an adversary. *arXiv preprint 2203.12592*, 2022.
- [10] Y. Chow, O. Nachum, and M. Ghavamzadeh. Path consistency learning in Tsallis entropy regularized MDPs. In *International Conference on Machine Learning (ICML)*, 2018.
- [11] P. Christodoulou. Soft actor-critic for discrete action settings. *arXiv 2019. arXiv preprint 1910.07207*, 2019.
- [12] F. Cipcigan, J. Booth, R. N. B. Ferreira, C. R. Dos Santos, and M. Steiner. Discovery of novel reticular materials for carbon dioxide capture using GFlowNets. *Digital Discovery*, 3(3): 449–455, 2024.
- [13] A. Currin, N. Swainston, P. J. Day, and D. B. Kell. Synthetic biology for the directed evolution of protein biocatalysts: navigating sequence space intelligently. *Chemical Society Reviews*, 44(5):1172–1239, 2015.
- [14] V.-A. Darvariu, S. Hailes, and M. Musolesi. Goal-directed graph construction using reinforcement learning. *Proceedings of the Royal Society A*, 477(2254):20210168, 2021.

- [15] S. E. Davis, S. Cremaschi, and M. R. Eden. Efficient surrogate model development: impact of sample size and underlying model dimensions. In *Computer aided chemical engineering*, volume 44, pages 979–984. Elsevier, 2018.
- [16] N. De Cao and T. Kipf. MolGAN: An implicit generative model for small molecular graphs. *arXiv preprint 1805.11973*, 2018.
- [17] T. Deleu, P. Nouri, N. Malkin, D. Precup, and Y. Bengio. Discrete probabilistic inference as control in multi-path environments. *Conference on Uncertainty in Artificial Intelligence (UAI)*, 2024.
- [18] E. Derman, M. Geist, and S. Mannor. Twice regularized MDPs and the equivalence between robustness and regularization. *Neural Information Processing Systems (NeurIPS)*, 2021.
- [19] Y. Du, T. Fu, J. Sun, and S. Liu. Molgensurvey: A systematic survey in machine learning models for molecule design. *arXiv preprint 2203.14500*, 2022.
- [20] B. Eysenbach and S. Levine. Maximum entropy RL (provably) solves some robust RL problems. *arXiv preprint 2103.06257*, 2021.
- [21] U. Gadot, E. Derman, N. Kumar, M. M. Elfatih, K. Levy, and S. Mannor. Solving non-rectangular reward-robust MDPs via frequency regularization. In *AAAI Conference on Artificial Intelligence*, 2024.
- [22] Y. Gan, Z. Zhang, and X. Tan. Stabilizing q learning via soft mellowmax operator. In *AAAI Conference on Artificial Intelligence*, 2021.
- [23] M. Geist, B. Scherrer, and O. Pietquin. A theory of regularized markov decision processes. In *International Conference on Machine Learning (ICML)*, 2019.
- [24] W. R. Gilks, S. Richardson, and D. Spiegelhalter. *Markov chain Monte Carlo in practice*. CRC press, 1995.
- [25] J. Gubernatis and T. Lookman. Machine learning in materials design and discovery: Examples from the present and suggestions for the future. *Physical Review Materials*, 2(12):120301, 2018.
- [26] T. Haarnoja, H. Tang, P. Abbeel, and S. Levine. Reinforcement learning with deep energy-based policies. In *International Conference on Machine Learning (ICML)*, 2017.
- [27] T. Haarnoja, A. Zhou, P. Abbeel, and S. Levine. Soft actor-critic: Off-policy maximum entropy deep reinforcement learning with a stochastic actor. In *International Conference on Machine Learning (ICML)*, 2018.
- [28] S. Huang, R. F. J. Dossa, C. Ye, J. Braga, D. Chakraborty, K. Mehta, and J. G. Araújo. CleanRL: High-quality single-file implementations of deep reinforcement learning algorithms. *Journal of Machine Learning Research*, 23(274):1–18, 2022. URL <http://jmlr.org/papers/v23/21-1342.html>.
- [29] H. Husain, K. Ciosek, and R. Tomioka. Regularized policies are reward robust. In *International Conference on Artificial Intelligence and Statistics (AISTATS)*, 2021.
- [30] G. N. Iyengar. Robust dynamic programming. *Mathematics of Operations Research*, 30(2): 257–280, 2005.
- [31] M. Jain, E. Bengio, A. Hernandez-Garcia, J. Rector-Brooks, B. F. Dossou, C. A. Ekbote, J. Fu, T. Zhang, M. Kilgour, D. Zhang, et al. Biological sequence design with GFlowNets. In *International Conference on Machine Learning (ICML)*, 2022.
- [32] M. Jain, T. Deleu, J. Hartford, C.-H. Liu, A. Hernandez-Garcia, and Y. Bengio. GFlowNets for AI-driven scientific discovery. *Digital Discovery*, 2(3):557–577, 2023.
- [33] M. Jiralerspong, B. Sun, D. Vucetic, T. Zhang, Y. Bengio, G. Gidel, and N. Malkin. Expected flow networks in stochastic environments and two-player zero-sum games. In *International Conference on Learning Representations (ICLR)*, 2024.

- [34] R. M. Karp. Reducibility among combinatorial problems. In *50 Years of Integer Programming 1958-2008: from the Early Years to the State-of-the-Art*, pages 219–241. Springer, 2009.
- [35] M. Kim, J. Ko, T. Yun, D. Zhang, L. Pan, W. Kim, J. Park, E. Bengio, and Y. Bengio. Learning to scale logits for temperature-conditional GFlowNets. *arXiv preprint 2310.02823*, 2023.
- [36] D. P. Kingma. Adam: A method for stochastic optimization. *arXiv preprint 1412.6980*, 2014.
- [37] V. I. Levenshtein et al. Binary codes capable of correcting deletions, insertions, and reversals. In *Soviet physics doklady*, volume 10, pages 707–710. Soviet Union, 1966.
- [38] K. Madan, J. Rector-Brooks, M. Korablyov, E. Bengio, M. Jain, A. C. Nica, T. Bosc, Y. Bengio, and N. Malkin. Learning GFlowNets from partial episodes for improved convergence and stability. In *International Conference on Machine Learning (ICML)*, 2023.
- [39] N. Malkin, M. Jain, E. Bengio, C. Sun, and Y. Bengio. Trajectory balance: Improved credit assignment in GFlowNets. *Neural Information Processing Systems (NeurIPS)*, 2022.
- [40] S. Mannor, D. Simester, P. Sun, and J. N. Tsitsiklis. Bias and variance in value function estimation. In *International Conference on Machine Learning (ICML)*, 2004.
- [41] S. Mohammadpour, E. Bengio, E. Frejinger, and P.-L. Bacon. Maximum entropy GFlowNets with soft q-learning. In *International Conference on Artificial Intelligence and Statistics*, 2024.
- [42] S. Mohammadpour, E. Frejinger, and P.-L. Bacon. Decoupling regularization from the action space. In *International Conference on Learning Representations (ICLR)*, 2024.
- [43] O. Nachum, M. Norouzi, K. Xu, and D. Schuurmans. Bridging the gap between value and policy based reinforcement learning. *Neural Information Processing Systems (NeurIPS)*, 2017.
- [44] M. Pirtskhalava, A. A. Armstrong, M. Grigolava, M. Chubinidze, E. Alimbarashvili, B. Vishnepolsky, A. Gabrielian, A. Rosenthal, D. E. Hurt, and M. Tartakovsky. DBAASP v3: database of antimicrobial/cytotoxic activity and structure of peptides as a resource for development of new therapeutics. *Nucleic acids research*, 49(D1):D288–D297, 2021.
- [45] M. L. Puterman. *Markov decision processes: Discrete stochastic dynamic programming*. John Wiley & Sons, 2014.
- [46] L. Richter, A. Boustati, N. Nüsken, F. Ruiz, and O. D. Akyildiz. Vargrad: A low-variance gradient estimator for variational inference. *Neural Information Processing Systems (NeurIPS)*, 2020.
- [47] J. Schulman, F. Wolski, P. Dhariwal, A. Radford, and O. Klimov. Proximal policy optimization algorithms. *arXiv preprint 1707.06347*, 2017.
- [48] T. Shen, M. Pandey, and M. Ester. Tacogfn: Target conditioned GFlowNet for drug design. In *NeurIPS 2023 Generative AI and Biology (GenBio) Workshop*, 2023.
- [49] D. Tiapkin, N. Morozov, A. Naumov, and D. P. Vetrov. Generative flow networks as entropy-regularized rl. In *International Conference on Artificial Intelligence and Statistics (AISTATS)*, 2024.
- [50] B. Trabucco, X. Geng, A. Kumar, and S. Levine. Design-bench: Benchmarks for data-driven offline model-based optimization. In *International Conference on Machine Learning (ICML)*, 2022.
- [51] H. Wang, T. Fu, Y. Du, W. Gao, K. Huang, Z. Liu, P. Chandak, S. Liu, P. Van Katwyk, A. Deac, et al. Scientific discovery in the age of artificial intelligence. *Nature*, 620(7972):47–60, 2023.
- [52] M. L. Waskom. seaborn: statistical data visualization. *Journal of Open Source Software*, 6(60): 3021, 2021. doi: 10.21105/joss.03021. URL <https://doi.org/10.21105/joss.03021>.
- [53] W. Wiesemann, D. Kuhn, and B. Rustem. Robust Markov decision processes. *Mathematics of Operations Research*, 38(1):153–183, 2013.

- [54] Z. Wu, K. E. Johnston, F. H. Arnold, and K. K. Yang. Protein sequence design with deep generative models. *Current opinion in chemical biology*, 65:18–27, 2021.
- [55] D. W. Zhang, C. Rainone, M. Peschl, and R. Bondesan. Robust scheduling with GFlowNets. *International Conference on Learning Representations (ICLR)*, 2023.
- [56] M. Zhou, Z. Yan, E. Layne, N. Malkin, D. Zhang, M. Jain, M. Blanchette, and Y. Bengio. PhyloGFN: Phylogenetic inference with generative flow networks. *International Conference on Learning Representations (ICLR)*, 2024.

## A Robustness-Regularization Duality

### A.1 Convex Analysis

Before proving our results, we briefly recall notions of convex analysis below [6].

**Definition A.1** (Convex conjugate). *Let a function  $f : \mathbb{R}^n \rightarrow \bar{\mathbb{R}}$  with domain  $\text{dom}(f) \subseteq \mathbb{R}^n$ . The convex conjugate of  $f$  is defined as*

$$f^*(y) := \sup_{x \in \text{dom}(f)} \langle x, y \rangle - f(x).$$

**Definition A.2** (Infimal convolution). *Given two functions  $f, g : \mathbb{R}^n \rightarrow \bar{\mathbb{R}}$ , the infimal convolution of  $f$  and  $g$  is defined as:*

$$[f \square g](x) := \inf_{z \in \mathbb{R}^n} \{f(x - z) + g(z)\}.$$

**Property A.1** (Operations on conjugate transforms). *Let two functions  $f_1, f_2 : \mathbb{R}^n \rightarrow \bar{\mathbb{R}}$  and a positive real number  $\omega > 0$ .*

- (i) *Defining  $g(x) := \omega f_1(x)$ , the convex conjugate of  $g$  satisfies  $g^*(y) = \omega f_1^*\left(\frac{y}{\omega}\right)$ .*
- (ii) *For  $\kappa \neq 0$  and  $h(x) := f_1(\kappa x)$ , the convex conjugate of  $h$  satisfies  $h^*(y) = f_1^*\left(\frac{y}{\kappa}\right)$ .*
- (iii) *The convex conjugate of the sum  $f_1 + f_2$  is the infimal convolution of their conjugates  $f_1^* \square f_2^*$ , namely:*

$$[f_1 + f_2]^*(y) = [f_1^* \square f_2^*](y), \quad \forall y \in \mathbb{R}^n.$$

### A.2 Application to policy divergence

For Shannon entropy and KL divergence, the convex conjugate can be derived in closed form and is known to be a logsumexp function, so we omit the proof [23, 18].

**Proposition A.1** (Shannon conjugate). *Define the negative Shannon entropy  $-H : \mathbb{R}^n \rightarrow \bar{\mathbb{R}}$  as  $[-H](x) := \sum_{i=1}^n x_i \log(x_i)$  over the simplex domain  $\Delta_n$ . It is a convex function, and its convex conjugate is the logsumexp:*

$$\text{LSE}_n(y) := \log \left( \sum_{i=1}^n e^{y_i} \right), \quad \forall y \in \mathbb{R}^n.$$

**Proposition A.2** (KL conjugate). *Let  $d \in \mathbb{R}^n$  be such that  $d > 0$  and define the KL-divergence function  $\text{KL}_d(x) := \sum_{i=1}^n x_i \log\left(\frac{x_i}{d_i}\right)$ ,  $\forall x \in \Delta_n$ . It is a convex function, and its convex conjugate is the weighted logsumexp:*

$$\text{WLSE}_{n,d}(y) := \log \left( \sum_{i=1}^n d_i e^{y_i} \right), \quad \forall y \in \mathbb{R}^n.$$

We are now interested in deriving the Fenchel conjugate of a convex combination of Shannon entropy and KL divergence. Its explicit form is described below.

**Proposition A.3** (Shannon-KL conjugate). *For any  $q \in [0, 1]$ , the convex combination  $(1 - q)(-H) + q\text{KL}_d$  satisfies:*

$$[(1 - q)(-H) + q\text{KL}_d](x) = \sum_{i=1}^n x_i \log \left( \frac{x_i}{(d_i)^q} \right), \quad \forall x \in \mathbb{R}^n.$$

*and admits as convex conjugate the function:*

$$[(1 - q)(-H) + q\text{KL}_d]^*(y) = \log \left( \sum_{i=1}^n (d_i)^q e^{y_i} \right), \quad \forall y \in \mathbb{R}^n.$$

*Proof.* The first statement comes from elementary algebra:

$$\begin{aligned}
[(1 - \mathbf{q})(-\mathbf{H}) + \mathbf{q}\text{KL}_d](x) &= (1 - \mathbf{q}) \sum_{i=1}^n x_i \log(x_i) + \mathbf{q} \sum_{i=1}^n x_i \log\left(\frac{x_i}{d_i}\right) \\
&= (1 - \mathbf{q} + \mathbf{q}) \sum_{i=1}^n x_i \log(x_i) - \mathbf{q} \sum_{i=1}^n x_i \log(d_i) \\
&= \sum_{i=1}^n x_i \log(x_i) - \sum_{i=1}^n x_i \log((d_i)^{\mathbf{q}}) \\
&= \sum_{i=1}^n x_i \log\left(\frac{x_i}{(d_i)^{\mathbf{q}}}\right) = \text{KL}_{d^{\mathbf{q}}}(x).
\end{aligned}$$

For the second statement, we simply apply Prop. A.2 to obtain that

$$[(1 - \mathbf{q})(-\mathbf{H}) + \mathbf{q}\text{KL}_d]^*(y) = \text{WLSE}_{n,d^{\mathbf{q}}}(y) = \log\left(\sum_{i=1}^n (d_i)^{\mathbf{q}} e^{y_i}\right).$$

A more involved proof would combine notions of infimal convolution with the respective conjugates of the two divergences. We omit it for brevity.  $\square$

### A.3 Proof of Thm. 4.1

We provide a slightly general proof below, with an arbitrary  $\epsilon_s$ -level set instead of just 0.

**Theorem A.1** (Fenchel-Robust Regularized MDP). *For any  $s \in \mathcal{S}$ , define the reward set*

$$\mathcal{R}_s := r_0(s, \cdot) + \{r_s \in \mathbb{R}^{\mathcal{A}} : f_s^*(-r_s) \leq \epsilon_s\},$$

*and the regularization function  $\Omega_s(\pi_s) := f_s(\pi_s) + \epsilon_s$ ,  $\forall s \in \mathcal{S}$ . Then, for any policy  $\pi \in \Pi$ ,  $T_{\mathcal{R}}^{\pi}v = T^{\pi,\Omega}v$ ,  $\forall v \in \mathbb{R}^{\mathcal{S}}$ , and  $v_{\mathcal{R}}^{\pi} = v^{\pi,\Omega}$ .*

*Proof.* First, we establish the support function of a set  $\tilde{\mathcal{R}}_s := \{r'_s \in \mathbb{R}^{\mathcal{A}} : f_s^*(r'_s) \leq \epsilon_s\}$  at any state  $s \in \mathcal{S}$ . By definition, for any policy  $\pi_s \in \Delta_{\mathcal{A}}$ , we have

$$\begin{aligned}
\max_{r'_s \in \tilde{\mathcal{R}}_s} \langle \pi_s, r'_s \rangle &= \max_{\{r'_s \in \mathbb{R}^{\mathcal{A}} : f_s^*(r'_s) \leq \epsilon_s\}} \langle \pi_s, r'_s \rangle \\
&= f_s(\pi_s) + \epsilon_s.
\end{aligned}$$

Next, we compute the robust Bellman operator associated with the uncertainty set  $\mathcal{R} = \times_s \mathcal{R}_s$ :

$$\begin{aligned}
T_{\mathcal{R}}^{\pi}v(s) &= \min_{r_s \in \mathcal{R}_s} r^{\pi}(s) + \gamma P^{\pi}v(s) \\
&= \min_{r_s \in r_0(s, \cdot) + \tilde{\mathcal{R}}_s} r^{\pi}(s) + \gamma P^{\pi}v(s) \\
&= r_0^{\pi}(s) + \min_{r'_s \in \tilde{\mathcal{R}}_s} \langle \pi_s, r'_s \rangle + \gamma P^{\pi}v(s) \\
&= r_0^{\pi}(s) - \max_{r'_s \in \tilde{\mathcal{R}}_s} \langle \pi_s, -r'_s \rangle + \gamma P^{\pi}v(s) \\
&= T_{r_0}^{\pi}v(s) - \max_{r'_s \in \tilde{\mathcal{R}}_s} \langle \pi_s, -r'_s \rangle.
\end{aligned}$$

It remains to compute

$$\begin{aligned}
\max_{r'_s \in \tilde{\mathcal{R}}_s} \langle \pi_s, -r'_s \rangle &= \max_{r'_s} \langle \pi_s, -r'_s \rangle \text{ s. t. } f_s^*(-r'_s) \leq \epsilon_s \\
&= \max_{\bar{r}_s} \langle \pi_s, \bar{r}_s \rangle \text{ s. t. } f_s^*(\bar{r}_s) \leq \epsilon_s
\end{aligned}$$

Employing the above expression of the support function enables us to write:

$$\max_{\bar{r}_s} \langle \pi_s, \bar{r}_s \rangle \text{ s. t. } f_s^*(\bar{r}_s) \leq \epsilon_s = f_s(\pi_s) + \epsilon_s$$

so that  $T_{\mathcal{R}}^{\pi}v = T^{\pi,\Omega}v$ ,  $\forall v \in \mathbb{R}^{\mathcal{S}}$ . The unique fixed point of each operator is  $v_{\mathcal{R}}^{\pi}$  and  $v^{\pi,\Omega}$ , respectively, which leads to the conclusion.  $\square$



Equation 6 comes from combining Thm. 4.1 with Prop. A.3. We can similarly obtain the uncertainty set resulting from KL and negative Shannon regularizations, based on their corresponding dual described in Sec. A.1. This leads us to the following table, summarizing the different regularizers used in this paper along with their corresponding uncertainty sets.

Table 1: Summary table of policy regularizers.

	Neg. Shannon	KL divergence	GSM	General convex
<b>Regularizer</b> $\Omega_s$	$-\mathcal{H}(\pi_s)$	$\text{KL}(\pi_s, d_s)$	$\frac{1}{\omega_s}(\mathbf{q}\text{KL}(\pi_s, d_s) + (1-\mathbf{q})(-\mathcal{H}(\pi_s)))$	$f_s(\pi_s) + \epsilon_s$
<b>Conjugate</b> $\Omega_s^*$	$\text{LSE}_{\mathcal{A}}(q_s)$	$\text{WLSE}_{\mathcal{A}, d_s}(q_s)$	$\omega_s^{-1} \text{WLSE}_{\mathcal{A}, d_s^{\mathbf{q}}}(\omega_s q_s)$	$f_s^*(q_s) - \epsilon_s$
<b>Reward Uncertainty</b>	$\{r_s : \Omega_s^*(-r_s) \leq 0\}$	$\{r_s : \Omega_s^*(-r_s) \leq 0\}$	$\{r_s : \Omega_s^*(-r_s) \leq 0\}$	$\{r_s : f_s^*(-r_s) \leq \epsilon_s\}$

#### A.4 Proof of Prop. 4.1

**Proposition A.4.** For all  $\mathbf{q} \in [0, 1]$ ,  $\Omega_s^{\mathbf{q}}(\pi_s) = \frac{1}{\omega_s} \text{KL}(\pi_s, d_s^{\mathbf{q}}) - \frac{1}{\omega_s} \log(Z_{\mathbf{q}}(d_s))$ , where  $Z_{\mathbf{q}}(d_s) := \sum_{a \in \mathcal{A}} d_s(a)^{\mathbf{q}}$  and  $d_s^{(\mathbf{q})} = d_s^{\mathbf{q}}/Z_{\mathbf{q}}(d_s)$  is the  $\mathbf{q}$ -tilted softmax distribution.

*Proof.* By definition,

$$\begin{aligned}
\omega_s \Omega_s^{\mathbf{q}}(\pi_s) &= [\mathbf{q} \text{KL}(\pi_s, d_s) + (1 - \mathbf{q})(-\mathcal{H}(\pi_s))] \\
&= \mathbf{q} \sum_{a \in \mathcal{A}} \pi_s(a) \log \left( \frac{\pi_s(a)}{d_s(a)} \right) + (1 - \mathbf{q}) \sum_{a \in \mathcal{A}} \pi_s(a) \log(\pi_s(a)) \\
&= -\mathbf{q} \sum_{a \in \mathcal{A}} \pi_s(a) \log(d_s(a)) + \sum_{a \in \mathcal{A}} \pi_s(a) \log(\pi_s(a)) \\
&= \sum_{a \in \mathcal{A}} \pi_s(a) \log \left( \frac{\pi_s(a)}{d_s(a)^{\mathbf{q}}} \right) \\
&= \sum_{a \in \mathcal{A}} \pi_s(a) \log \left( \frac{\pi_s(a)}{d_s(a)^{\mathbf{q}}/Z_{\mathbf{q}}(d_s)} \right) - \sum_{a \in \mathcal{A}} \pi_s(a) \log(Z_{\mathbf{q}}(d_s)) \\
&= \sum_{a \in \mathcal{A}} \pi_s(a) \log \left( \frac{\pi_s(a)}{d_s(a)^{\mathbf{q}}/Z_{\mathbf{q}}(d_s)} \right) - \log(Z_{\mathbf{q}}(d_s)),
\end{aligned}$$

which yields the desired result.  $\square$

## B Multi-step uncertainty sets

While Fig. 3 examines the case of uncertainty sets for a single step, we now seek to explore the values that can be taken by  $\delta_i$  throughout a trajectory and how this affects the final uncertainty set. For the entropic regularizer, if  $\omega_s$  is the same for all  $s$ , then  $\mathcal{R}_{s_i}$  is the same at every state. However, the final uncertainty set  $\mathcal{R}$  for an object  $x = s_1 s_2 \dots s_n$  is given by  $\sum_i \mathcal{R}_{s_i}$  (i.e. the Minkowski sum of the individual uncertainty sets).

We extend the binary generation example to a DCG consisting of a sequence generation task with two tokens (i.e. a binary tree) and length  $d$ . Then, using Prop B.1, in Fig. 7, we illustrate how the sum of uncertainty sets change as the depth of the tree increases for different operators.

**Proposition B.1.** *For a convex regularizer  $f$  and associated robust set  $\mathcal{R}_f = \{\delta \in \mathbb{R}^{|\mathcal{A}|} : f^*(\delta) \leq 0\}$ , we have that:*

$$\sum_{i=1}^k \mathcal{R}_f = \{r \in \mathbb{R}^{|\mathcal{A}|} : kf^*\left(\frac{r}{k}\right) \leq 0\}. \quad (10)$$

*Proof.* We seek to show that, for a given  $r \in \mathbb{R}^{|\mathcal{A}|}$ , there exists  $\delta_1, \delta_2 \dots \delta_k$  such that  $\sum_{i=1}^k \delta_i = r$  and  $\delta_i \in \mathcal{R}_f$  if and only if  $kf^*\left(\frac{r}{k}\right) \leq 0$ .

[ $\Rightarrow$ ] Since  $f$  is convex, so is  $f^*$ . Thus, using Jensen’s inequality, we get that:

$$kf^*\left(\frac{r}{k}\right) = kf^*\left(\frac{\sum_i \delta_i}{k}\right) \leq \sum_i f^*(\delta_i) \leq 0,$$

where the last inequality stems from  $\delta_i \in \mathcal{R}_f \Rightarrow f^*(\delta_i) \leq 0$ .

[ $\Leftarrow$ ] Taking  $\delta_i = \frac{r}{k}$  for all  $\delta_i$ , we have that  $\sum_i \delta_i = r$ . Then,  $kf^*\left(\frac{r}{k}\right) \leq 0 \Rightarrow \forall i : f^*(\delta_i) = f^*\left(\frac{r}{k}\right) \leq 0$  and thus  $\delta_i \in \mathcal{R}_f$ .  $\square$

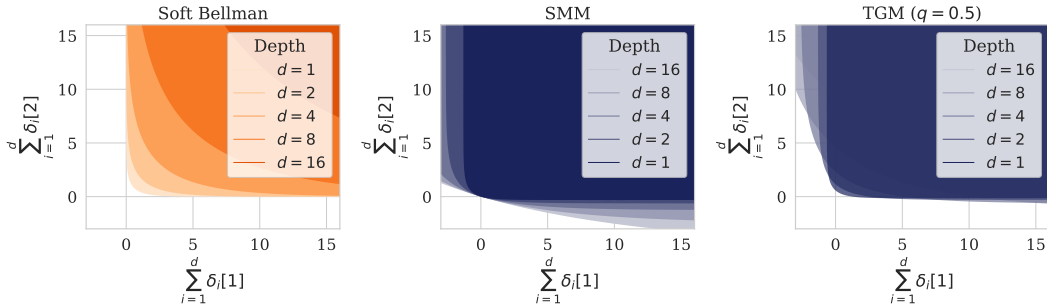


Figure 7: Illustration of sum of uncertainty sets along a trajectory. (Left) The final uncertainty set shifts farther away from  $(0, 0)$  as we increase  $d$ . As such, for objects that are deeper in the tree, the operator is only robust to them having much higher reward than their proxy evaluation. This behavior provides an alternative viewpoint for the preference of the soft Bellman operator for longer objects. (Middle) On the other hand, the SMM operator stays centered around  $(0, 0)$  and becomes increasingly robust to decreases in rewards. (Right) The final uncertainty set of the GM operator stays close to  $(0, 0)$  and is robust to some decreases in reward.

## C Trajectory General Mellowmax

**Notation:** We denote by  $\text{Ch}(s)$  the set of possible actions from state  $s$ .  $\sigma_\tau(Q_s) := \frac{e^{\tau Q_s}}{\sum_{a' \in \text{Ch}(s)} e^{\tau Q_s[a']}}$  is the softmax with inverse temperature  $\tau$ . For a DCG and a given state  $s$ , we denote by  $s'_a$  the state reached by taking action  $a$  (unique since transitions are deterministic). We denote by  $E$  the set of edges in  $\mathcal{G}$ , each of which represents a transition  $(s, a, s'_a)$ . For any state  $s$ ,

$$\forall a \in \text{Ch}(s) : Q_s[a] := v_{s_a} + r(s, a).$$

Finally, for convenience, we denote

$$\begin{aligned} g(Q_s, a) &:= \frac{1}{\omega} \log \sigma_{\mathbf{q}\alpha + \omega}(Q_s)[a] - \mathbf{q} \log \sigma_\alpha(Q_s)[a], \\ g^*(Q_s) &:= \frac{1}{\omega} \log \langle \sigma_\alpha(Q_s)^\mathbf{q}, e^{\omega Q_s} \rangle. \end{aligned}$$

### C.1 Proof of optimality

**Proposition C.1.** *In a DCG  $(\mathcal{G}, r)$ , for any state  $s$ ,*

$$v_s^* := \max_{\pi_s} \langle \pi_s, Q_s \rangle - \frac{1}{\omega} \Omega_{\sigma_\alpha(Q_s), s}^\mathbf{q}(\pi_s) = \frac{1}{\omega} \log \langle \sigma_\alpha(Q_s)^\mathbf{q}, e^{\omega Q_s} \rangle = g^*(Q_s), \quad (11)$$

and

$$\pi_s^* = \sigma_{\mathbf{q}\alpha + \omega}(Q_s). \quad (12)$$

is the unique maximizer of the state-wise regularized problem.

*Proof.* Unlike the case of a generic  $\pi$ , (11) is not a convex conjugate since  $Q_s$  appears in both the dot product and  $\Omega$ . Nonetheless,  $\Omega$  is still convex in  $\pi$ . Thus, similarly to [43], we consider the Lagrangian:

$$L(\pi_s, \lambda) = \langle \pi_s, Q_s \rangle - \frac{1}{\omega} \Omega_{\sigma_\alpha(Q_s), s}^\mathbf{q}(\pi_s) + \lambda(1 - \langle \mathbf{1}, \pi_s \rangle).$$

Since  $\Omega$  is convex, the overall function to optimize is concave. Given that Slater's condition holds, the KKT conditions are both sufficient and necessary for optimality. Due to the lack of cycle in DCGs, we have that  $\nabla_{\pi_s} Q_s = 0$ . Hence, the KKT conditions yield the following system of equations:

$$0 = Q_s - \frac{1}{\omega} (\mathbf{q}[\log \pi_s - \log \pi_{Q_s} + 1] + (1 - \mathbf{q})[\log \pi_s + 1]) - \lambda \quad (13)$$

$$1 = \langle \pi_s, \mathbf{1} \rangle \quad (14)$$

where we denote  $\pi_{Q_s} := \sigma_\alpha(Q_s)$ . Solving for  $\pi_s$  in the first, we get that the optimal policy  $\pi_s^*$  is given by:

$$\pi_s^* = \exp([Q_s - \lambda]\omega + \mathbf{q} \log \pi_{Q_s} - 1)$$

which ensures that  $\pi_s \geq 0$ . Replacing the above in (14), we have that:

$$\lambda^* = \frac{1}{\omega} \left( \log \sum_{a \in \text{Ch}(s)} e^{(\alpha \mathbf{q} + \omega) Q_s[a]} - \mathbf{q} \log \sum_{a \in \text{Ch}(s)} e^{\alpha Q_s[a]} \right) = \frac{1}{\omega} (\log \langle \sigma_\alpha(Q_s)^\mathbf{q}, e^{\omega Q_s} \rangle - 1).$$

We note the similarity of  $\lambda^*$  and the maximal value (11). Plugging  $\lambda^*$  back in to  $\pi_s^*$ , we get

$$\pi_s^* = \sigma_{\mathbf{q}\alpha + \omega}(Q_s). \quad (12)$$

Finally, plugging  $\pi_s^*$  in  $\langle \pi_s, Q_s \rangle - \frac{1}{\omega} \Omega_{\sigma_\alpha(Q_s), s}^\mathbf{q}(\pi_s)$  with some straightforward algebraic manipulations, we obtain (11). Since both the KL divergence and the negative entropy are strictly convex, (12) is the unique maximizer.  $\square$

**Corollary C.1.** *For any DCG  $(\mathcal{G}, \Phi)$  setting  $v_x^* = 0$  for all  $x \in \mathcal{X}$  yields unique optimal value/policy functions  $(v^*, \pi^*)$  for the GM operator.*

*Proof.* We show this by induction on an inverse topological sorting  $s_0, s_1 \dots, s_n$  of the states of  $\mathcal{G}$ . For a state with no children, the optimal value is uniquely defined to be 0 and there is no policy. Then, assume each state  $s_i, i < N$  has a unique optimal value/policy. By the properties of the topological sorting, all the children of  $s_N$  have a unique optimal value/policy. Then, by Prop. C.1,  $(v_{s_N}^*, \pi_{s_N}^*)$  is also uniquely defined.  $\square$

**Lemma C.1.** For any  $Q_s$  and  $a$ , we have that

$$g(Q_s, a) = Q_s[a] - g^*(Q_s). \quad (15)$$

*Proof.* By simple algebra,

$$\begin{aligned} g(Q_s, a) &= \frac{1}{\omega} (\log \sigma_{\mathbf{q}\alpha + \omega}(Q_s)[a] - \mathbf{q} \log \sigma_\alpha(Q_s)[a]) \\ &= \frac{1}{\omega} ((\mathbf{q}\alpha + \omega)Q_s[a] - \mathbf{q}\alpha Q_s[a]) \\ &\quad - \frac{1}{\omega} \left( \log \sum_{a' \in \text{Ch}(s)} e^{(\mathbf{q}\alpha + \omega)Q_s[a']} - \log \left[ \sum_{a' \in \text{Ch}(s)} e^{\alpha Q_s[a']} \right]^\mathbf{q} \right) \\ &= \frac{1}{\omega} (\omega Q_s[a]) - \frac{1}{\omega} \log \left[ \sum_{a' \in \text{Ch}(s)} \frac{e^{\mathbf{q}\alpha Q_s[a']} e^{\omega Q_s[a']}}{\left( \sum_{a' \in \text{Ch}(s)} e^{\alpha Q_s[a']} \right)^\mathbf{q}} \right] \\ &= Q_s[a] - \frac{1}{\omega} (\log \langle \sigma_\alpha(Q_s)^\mathbf{q}, e^{\omega Q_s} \rangle) \\ &= Q_s[a] - g^*(Q_s) \end{aligned}$$

$\square$

**Lemma C.2.** For any state  $s$  in a DCG, the following are equivalent:

$$\sigma_{\alpha\mathbf{q} + \omega}(\tilde{Q}_s) = \arg \max_{\pi_s} \langle \pi_s, Q_s^* \rangle - \frac{1}{\omega} \Omega_{\sigma_\alpha(Q_s^*), s}^\mathbf{q}(\pi_s), \quad (16)$$

$$\forall a \in \text{Ch}(s) : v_{s'_a}^* = v_s^* + g(\tilde{Q}_s, a) - r(s, a). \quad (17)$$

*Proof.*

[ (16)  $\Rightarrow$  (17) ] Since  $\pi_s^*$  is unique, by (16) and (12), we have that  $\sigma_{\alpha\mathbf{q} + \omega}(\tilde{Q}_s) = \sigma_{\alpha\mathbf{q} + \omega}(Q_s^*)$ . Then, for any  $a \in \text{Ch}(s)$ , we have that:

$$\begin{aligned} v_s^* + g(\tilde{Q}_s, a) &= v_s^* + \frac{1}{\omega} \left( \log \sigma_{\alpha\mathbf{q} + \omega}(\tilde{Q}_s)[a] - \mathbf{q} \log \sigma_\alpha(\tilde{Q}_s)[a] \right) \\ &= \frac{1}{\omega} \left( \log \langle \sigma_\alpha(Q_s^*)^\mathbf{q}, e^{\omega Q_s^*} \rangle + \log \sigma_{\alpha\mathbf{q} + \omega}(Q_s^*)[a] - \mathbf{q} \log \sigma_\alpha(Q_s^*)[a] \right) \quad \text{Using (11).} \\ &= \frac{1}{\omega} \left( \log \frac{\sum_{a' \in \text{Ch}(s)} e^{(\mathbf{q}\alpha + \omega)Q_s^*[a']}}{\sum_{a' \in \text{Ch}(s)} e^{\alpha Q_s^*[a']}} + \log \sigma_{\alpha\mathbf{q} + \omega}(Q_s^*)[a] - \mathbf{q} \log \sigma_\alpha(Q_s^*)[a] \right) \\ &= \frac{1}{\omega} \left( \log e^{(\mathbf{q}\alpha + \omega)Q_s^*[a]} - \mathbf{q} \log e^{\alpha Q_s^*[a]} \right) \\ &= Q_s^*[a] \\ &= v_{s'_a}^* + r(s, a) \quad \text{Using the definition of } Q_s[a]. \end{aligned}$$

[ (16)  $\Leftarrow$  (17) ] For any  $a \in \text{Ch}(s)$ , we have that:

$$\begin{aligned} v_{s'_a}^* &= v_s^* + g(\tilde{Q}_s, a) - r(s, a) \\ \iff v_{s'_a}^* &= v_s^* + \tilde{Q}_s[a] - g^*(\tilde{Q}_s) - r(s, a) \quad \text{Using (15)} \\ \iff v_s^* - g^*(\tilde{Q}_s) &= Q_s^*[a] - \tilde{Q}_s[a] \end{aligned}$$

Since the above equality holds for all actions and  $v_s^*$  and  $g^*(\tilde{Q}_s)$  do not depend on  $a$ , we have that  $Q_s^*[a] - \tilde{Q}_s[a]$  must be equal for all actions. Thus,  $\forall a \in \text{Ch}(s) : Q_s^*[a] - \tilde{Q}_s[a] = c$  which implies

$$\tilde{Q}_s[a] = Q_s^*[a] - c, \quad (18)$$

for some action independent value  $c$ . Finally, we have

$$\sigma_{\alpha q + \omega}(\tilde{Q}_s) = \sigma_{\alpha q + \omega}(Q_s^* - c) = \sigma_{\alpha q + \omega}(Q_s^*),$$

by the properties of the softmax.  $\square$

## C.2 Proof of Theorem 5.1

**Theorem C.1** (Trajectory GM). *For any DCG  $(\mathcal{G}, \Phi)$ , let  $(v^*, \pi^*)$  be the unique optimal value/policy functions for the GM operator with  $v_x^* = 0$  for all  $x \in \mathcal{X}$ . Then, for a given  $Q$ -function  $\tilde{Q}$ ,*

$$\sigma_{\alpha q + \omega}(\tilde{Q}_s) = \arg \max_{\pi_s} \langle \pi_s, Q_s \rangle - \frac{1}{\omega} \Omega_{\sigma_{\alpha}(Q_s), s}(\pi_s), \quad (8)$$

*holds for all states  $s$  if and only if*

$$v_0^* + \sum_{i=0}^n \underbrace{\frac{1}{\omega} \left( \log \sigma_{\alpha q + \omega}(\tilde{Q}_{s_i})[a_i] - q \log \sigma_{\alpha}(\tilde{Q}_{s_i})[a_i] \right)}_{g(\tilde{Q}_{s_i}, a_i)} - r(s_i, a_i) = 0, \quad (9)$$

*holds for all full trajectories  $s_0 \xrightarrow{a_0} \dots \xrightarrow{a_{n-1}} s_n \xrightarrow{a_n} x$  in the DCG.*

*Proof.* Similarly to [43], we aim to show that optimality implies consistency and vice versa. A refresher of relevant notation can be found at the start of App. C.

**Optimality implies consistency** [(8)  $\Rightarrow$  (9)] From Lemma C.2, for any given trajectory, we have that (17) holds for all transitions in the trajectory. Then, (9) follows straightforwardly by expanding (17) over that trajectory in a recursive manner.

**Consistency implies optimality** [(8)  $\Leftarrow$  (9)] Consider an inverse topological sorting  $s^1, s^2 \dots s^M$  of  $\mathcal{G}$  such that for any state  $s^i$ , any child  $s^j$  of  $s^i$  has index  $j < i$ .

Now, we seek to show by induction over this sorting that the following holds for any state  $s$  and subtrajectory  $s_0 \rightarrow s_1 \dots \rightarrow s_n \rightarrow s$  ending in  $s$ :

$$v_0^* + \sum_{i=0}^n \frac{1}{\omega} \left( \log \sigma_{\alpha q + \omega}(\tilde{Q}_{s_i})[a_i] - q \log \sigma_{\alpha}(\tilde{Q}_{s_i})[a_i] \right) - r(s_i, a_i) = v_s^*. \quad (19)$$

For the base case  $s^1$ ,  $s^1$  must be a leaf and belong to  $\mathcal{X}$ . Then, by assumption  $v_{s^1} = 0$  and (19) holds by (9). Now, suppose that (19) holds for any  $s^i$ ,  $i < N$ . Then, by the definition of the sorting, for all  $a \in \text{Ch}(s^N)$ , (19) holds for  $s_a$  where  $s^N \xrightarrow{a} s_a$ .

Let  $s_0 \rightarrow s_1 \dots \rightarrow s_n \rightarrow s^N$  be a trajectory ending in  $s^N$ . From the induction hypothesis,  $\forall a \in \text{Ch}(s) :$

$$\begin{aligned} v_0^* + \sum_{i=0}^n g(\tilde{Q}_{s_i}, a_i) - r(s_i, a_i) + g(\tilde{Q}_{s^N}, a) - r(s^N, a) &= v_{s_a}^* \\ v_0^* + \sum_{i=0}^n g(\tilde{Q}_{s_i}, a_i) - r(s_i, a_i) - g^*(\tilde{Q}_{s^N}) &= Q_{s^N}^*[a] - \tilde{Q}_{s^N}[a] \quad \text{Using (15).} \end{aligned}$$

Similarly to the proof of Lemma C.1, we have that the LHS is independent of  $a$  but must be equal to  $Q_{s^N}^*[a] - \tilde{Q}_{s^N}[a]$  for all  $a$ . As such, we are guaranteed

$$\tilde{Q}_{s^N}[a] = Q_{s^N}^*[a] - c$$

for some action independent value  $c$  and all  $a \in \text{Ch}(s^N)$ . Then, it is straightforward to compute  $g^*(\tilde{Q}_{s^N}) = g^*(Q_{s^N}^* - c) = g^*(Q_{s^N}^*) - c$ . Plugging both back in and canceling  $c$ , we get

$$v_0^* + \sum_{i=0}^n g(\tilde{Q}_{s_i}, a_i) - r(s_i, a_i) = g^*(Q_{s^N}^*) = v_{s^N}^*$$

and the induction is complete. Finally, it remains to show that  $\sigma_{\alpha q + \omega}(\tilde{Q}_s)$  is optimal for all  $s$ . If  $s$  has no children, optimality holds trivially. If  $s$  has at least one child  $a$ , take a trajectory  $s_0 \rightarrow s_1 \dots \rightarrow s_n \rightarrow s$  ending in  $s$ . From (19), we have that both:

$$\begin{aligned} v_0^* + \sum_{i=0}^n g(\tilde{Q}_{s_i}, a_i) - r(s_i, a_i) &= v_s^* \\ \forall a \in \text{Ch}(s) : v_0^* + \sum_{i=0}^n g(\tilde{Q}_{s_i}, a_i) - r(s_i, a_i) + g(\tilde{Q}_s, a) - r(s, a) &= v_{s_a}^*. \end{aligned}$$

By subtracting the first from the second, we get that,  $\forall a \in \text{Ch}(s)$ :

$$\begin{aligned} g(\tilde{Q}_s, a) - r(s, a) &= v_{s_a}^* - v_s^* \\ v_s^* + g(\tilde{Q}_s, a) - r(s, a) &= v_{s_a}^*. \end{aligned}$$

By Lemma C.2,  $\sigma_{\alpha q + \omega}(\tilde{Q}_s)$  is thus optimal at  $s$  and we are done.  $\square$

## D Experimental details

### D.1 Algorithms

We follow most of the hyperparameter decisions of [39]. For each method, we train a transformer with 3 layers, 8 attention heads and an embedding dimension of 64. We set dropout to 0.1 and use causal masking. Each output head uses a fully-connected network with 2 hidden layers of dimensions 256.

We use weight decay of  $10^{-4}$  and use gradient clipping with a threshold of 10 to help stabilize training at higher  $\beta$  values. When generating samples for training, we use a policy corresponding to a mixture of the method’s policy and a uniform policy (with weight 0.01). Each method is trained with Adam [36] with  $\epsilon = 10^{-5}$ .

**TGM/GFN:** Since GFNs correspond to a specific hyperparameter setting for TGM, training details are essentially identical between the two methods. Both methods are trained online with a batch size of 16 trajectories and have a single head that outputs logits. We sample trajectories by taking the tempered softmax of the logits, using the temperature  $\alpha q + \omega$  from the optimal policy (12). For GFNs,  $\omega$  affects the sampling policy but *not the actual training objective* as this ensures the network is learning the actual GFN objective.

**SAC:** For SAC, we use three networks: two Q networks (to reduce overestimation bias) and a policy network, following the implementation of [11, 28]. We use a replay buffer of size 100 000 and a batch size of 1 024 transitions. Generation/training is adjusted to have a replay ratio of 1.0. The entropy coefficient is fixed at  $1/\omega$  and we use target networks (for the Q networks) which get updated every 10 iterations.

**PPO:** For PPO, we use two networks: a policy network and a value network, following the implementation of [28]. We follow the hyperparameter settings of [28] and use a generalized advantage estimator  $\lambda$  of 0.95. The clipping epsilon is 0.1 and the value coefficient is 0.5. During online training, 16 trajectories are generated and the resulting transitions are split into 4 minibatches for training. The entropy coefficient is set to  $1/\omega$ .

### D.2 Sequences

For each sequence generation task, we add the following 3 tokens to the vocabulary: BOS, PAD, EOS. Sequences are padded to be of length equal to the maximum length for the task with an added BOS, EOS. Sequences look like the following:  $[\text{BOS}, x_1, \dots, x_n, \text{PAD}, \dots, \text{PAD}, \text{EOS}]$ . When generating sequences, they start with BOS and tokens are added until a terminating action is chosen, at which point PAD/EOS are added automatically. The terminating action is masked until the task’s minimum length is reached.

### D.3 Synthetic tasks

**TF-Bind-8.** Hyperparameters are as described in the paper. We sample 10 000 sequences for each method using their respective optimal policy. Fig. 4 is the kernel density estimate computed using these samples with the default parameters used by seaborn [52].

**Bit sequence.** We use  $n = 120$  and  $k = 8$  with  $M = 60$  modes and force sequences to be of length 120 through action masking. The modes are sampled randomly and fixed across runs to ensure there is no variation from certain runs having harder to find modes. Each method is trained for 200 000 samples.

### D.4 Biological sequence design

For each task, once the proxy reward model is trained, we compute the mean and standard deviation of the logits on the validation set. Then, we use the following normalized value as reward

$$r(x) = \beta \Phi(x) = \beta \frac{\phi(x) - \mu_{\text{val}}}{\sigma_{\text{val}}}, \quad (20)$$

where  $\phi(x)$  is the logit output by the trained model. To train the proxy reward models, we follow the hyperparameters used by [39].

**UTR:** Using the described dataset, we train a transformer with 4 layers, 8 attention heads and an embedding dimension of 64. 80% of the data is used for training and the rest for validation. We train for 250 epochs with early stopping (using a patience of 15). The learning rate is set to  $10^{-4}$  and we use a batch size of 128 and weight decay of  $1\text{e-}6$ . We set both the minimum and maximum length to 50 since all sequences in the dataset are of length 50.

**AMP:** We use the same hyperparameters for training the model as UTR. Since the dataset has sequences of variable length, we set the minimum length to 14 and the maximum length to 60. Unlike the other tasks, the model is trained for binary classification and we use the logit passed to the sigmoid as  $\phi(x)$ .

**GFP:** GFP is the largest task. We train a transformer with 3 layers, 8 attention heads and an embedding dimension of 128. Since all sequences are of length 237, we set both the minimum length and maximum length to 237.

#### D.4.1 Evaluation

For evaluation of the mean mode reward, we sweep over inverse temperature modifiers  $t \in \{0.005, 0.01, 0.02, 0.05, 0.1, 0.2, 0.5, 1, 2, 5\}$  (i.e. if the regular sampling policy was  $\pi \propto e^{\tau x}$ , we sample using  $\pi' \propto e^{\tau t x}$ ) and generate 512 samples for each. We then aggregate the samples and greedily find the top 100 samples such that they are at least at distance  $\delta$  of each other. We use the Levenshtein edit distance as metric [37] and set  $\delta = 0.25 \cdot \frac{\text{minLen} + \text{maxLen}}{2}$  (i.e.  $\delta = 13$  for UTR,  $\delta = 10$  for AMP and  $\delta = 60$  for GFP). The constraint can be roughly interpreted as requiring at least 25% of a sequence to be different for it to be considered distinct.

#### D.5 Compute resources

Experiments were conducted on a cluster with a mix of GPUs. All experiments were run using jobs that requested 1xL40s, 24G of RAM and 4 CPUs with the cluster allowing dozens of jobs to be run in parallel. Overall, the experiments (including all the hyperparameter sweeps, baselines and various seeds) used roughly:

- **Bit Sequence:** 35 GPU hours.
- **UTR:** 48 GPU hours.
- **AMP:** 48 GPU hours.
- **GFP:** 300 GPU hours.

for a total of roughly  $\approx 20$  GPU days. In particular, the entire codebase uses Jax [8] and a parallelized environment allowing for fast generation. Since we use transformers, training on a generated trajectory for TGM/GFNs only requires a single forward/backward pass. This significantly speeds up training (roughly 4x faster) compared to the PPO/SAC baselines which operate on individual transitions (though there are potential engineering optimizations to improve the speed of these baselines).



## **E Broader impact**

The purpose of this work is algorithmic in nature and we do not aim to produce actual applicable models. Nonetheless, the ideas in this work could potentially be used to improve the training of models used in protein or other biological sequence design applications. While there are numerous beneficial applications for these types of models, they could also be used to design sequences that could eventually be harmful to humans. This harm could come from bad actors or even accidentally by over-optimizing to a single metric (e.g. antimicrobial resistance) and not considering potential harmful effects on the body. The extension of this work to multi-objective settings is a fruitful direction for future work.

In addition, the contribution of this work also has applications in language (another sequence design task). As such, it both has the potential to improve the performance of large language models (LLMs) on both useful and nefarious tasks. Given the recent improvements in abilities of these models, this potential effect is especially relevant.